Benchmark and optimization of AlphaFold structures based virtual screening strategy

Yanfei Peng[1], Xia Wu[1], Liang Lin[1], Zhiluo Deng[2*], Limin Zhao[1*], Hao Ke[1*]

[1] Human Aging Research Institute (HARI) and School of Life Science, Nanchang University, and Jiangxi Key Laboratory of Human Aging, Nanchang, 330031 Jiangxi China

[2] Department for Computational Biology of Infection Research, Helmholtz Center for Infection Research, Braunschweig, Germany; Braunschweig Integrated Centre of Systems Biology (BRICS), Technische Universität Braunschweig, Braunschweig, Germany;

* Corresponding authors:

Zhiluo Deng, Tel: +49 531-391-55273, E-mail: Zhiluo.Deng@helmholtz-hzi.de

Limin Zhao, Tel: +86 181-8600-5898, E-mail: zhaolimin@ncu.edu.cn

Hao Ke, Tel: +86 135-1874-2153, E-mail: kehao@ncu.edu.cn

Abstract

Recent advancements in artificial intelligence such as AlphaFold, have enabled more accurate prediction of protein three-dimensional structure from amino acid sequences. This has attracted significant attention, especially for the application of AlphaFold in drug discovery. Moreover, how to take full advantage of AlphaFold to assist with virtual screening remains elusive. We comprehensively evaluated the AlphaFold structures of 51 selected targets from the DUD-E database in virtual screening. Our

analyses show that the virtual screening performance of about 35% of the AlphaFold structures was equivalent to that of DUD-E structures, and about 25% of the AlphaFold structures yielded better results than the DUD-E structures. Remarkably, for the 23 targets, AlphaFold structures produced slightly better results than the Apo structures. Moreover, we developed a new consensus scoring method based on Z-score standardization and exponential function, which showed improved screening performance compared to traditional scoring methods. By implementing a multi-stage virtual screening process and the new consensus scoring method, we were able to improve the speed of virtual screening by about nine times without compromising the enrichment factor. Overall, our results provide insights into the potential use of AlphaFold in drug discovery and highlight the value of consensus scoring and multi-stage virtual screening.

Key words: AlphaFold, virtual screening, high-throughput docking, consensus scoring, multi-stage virtual screening

Introduction

AlphaFold is deep learning based program that can predict the three-dimensional structure of proteins from amino acid sequences. It is one of the low-cost computing methods to obtain highly accurate protein structures[1]. Currently, the AlphaFold protein structure database contains over 200 million entries, covering the human proteome and the proteome of 47 other important organisms crucial to research and global health. The availability of large numbers of easily accessible and highly accurate protein structures has made AlphaFold a valuable resource for research fields related to protein structure, particularly for protein research that lacks experimental structure information[2].

Several studies have explored the use of AlphaFold protein structure for drug discovery[3–5]. A few recent studies evaluated the performance of AlphaFold protein

structure in virtual screening. Wong et al. evaluated the effectiveness of AlphaFold protein structure to predict the binding affinity of 296 E. coli proteins and 218 small molecules with known antibacterial activity, and compared the results to the experimental structure of 12 proteins[6]. Scardino et al. assessed the performance of the structure in the PDB database and AlphaFold structure in virtual screening using four docking software and ECR (Exponential Consensus Ranking, based on ranking) on 16 protein targets, and the consensus score of PRC (Pose/Ranking Consensus, based on docking pose and ranking)[7]. Zhang examined the efficiency of Holo, Apo and AlphaFold structures in virtual screening for 28 targets et al. with Glide molecular docking method[8]. Alon, et al. found that although the AlphaFold structure of σ2 receptor is very similar to the crystal structure, the score of small molecule compounds with the AlphaFold structure is lower than that of the crystal structure[9].

Virtual screening based on molecular docking is a widely used method in computer-aided drug design. With scoring function, molecular docking can effectively identify small molecules that interact with the ligand binding pocket of receptor protein. Numerous studies have reported the use of molecular docking based virtual screening to discover inhibitors and agonists of target proteins[9–12]. Virtual screening can effectively reduce the cost of drug discovery and accelerate the process. There are many different molecular docking methods widely used in virtual screening, including AutoDock Vina[13,14], Qvina2[15], idock[16], ICM[17], Glide[18], Gold[19], etc. However, molecular docking still has high false positive rate which limits its use in drug discovery. Some recent studies have used the consensus scoring method to integrate the score reported by different docking software to reduce the false positive rate and improve the enrichment factor[20,21]. Other studies have even takes into account the docking pose in consensus scoring, which can further improve the performance of the virtual screening [22–24]. Therefore, further optimization of the consensus scoring method could be of great significance for improving the value of AlphaFold in virtual screening.

With the rapid expansion of the small molecule library for virtual screening, for example, the ZINC database has provided more than 120 million purchasable drug-

like compounds[25], large-scale virtual screening plays an increasingly important role in drug discovery. However large-scale virtual screening requires a substantial amount of computing resources. To reduce the runtime and save computing resources, the multi-stage screening method has been used in large-scale virtual screening. Gorculla et al. conducted a large-scale screening with 1.3 billion compounds using a multi-stage screening method. In the first stage, Qvina2 was used for rapid screening with a low accuracy. In the second stage, 13 residues of the receptor were considered flexible, and AutoDock Vina and Smina Vinardo were used to re-score the top 3 million compounds from the first stage with a higher accuracy[10].

Protein structure can be categorized into Holo structure and Apo structure based on the presence of small molecules in the binding pocket. Holo structures have small molecules in the binding pocket, while Apo structures do not. Previous studies have shown that the category of the protein structure has a significant impact on virtual screening, and the results of Holo structure is generally better than that of Apo structure [26,27].

To comprehensively evaluate the impact of using AlphaFold protein structures, Holo and Apo structures on virtual screening, we selected 51 protein targets from the widely used DUD-E database[28] and more than 400,000 small molecules. A novel consensus scoring function was developed to achieve a lower false discovery rate. In the benchmark, various molecular docking software, scoring functions, and consensus scoring including the novel consensus scoring method were used. Our analyses show that the virtual screening performance of about 35% of the AlphaFold structures was equivalent to that of DUD-E structures, and about 25% of the AlphaFold structures yielded better results than the DUD-E structures. Remarkably, for the 23 targets, AlphaFold structures produced slightly better results than the Apo structures. Notably, the new consensus scoring method is superior to the traditional scoring method and can be used to design a multi-stage virtual screening process that improves the virtual screening speed by about 9 times without compromising the enrichment factor EF1%.

Results

Virtual screening based on protein structure in DUD-E database and AlphaFold

With autodock4 scoring function, all the metrics did not show substantial difference between DUD-E protein structures and AlphaFold protein structures (Fig. 1b, Fig. 1c) (p-value for logAUC between DUD-E and AlphaFold is 0.081). However, with the other scoring functions, DUD-E structures performed better than AlphaFold structures overall in terms of all metrics except for AUC (Fig. 1c). For idock the EF1% was 6.342 ± 8.808 for DUD-E structure and 3.985 ± 5.191 for AlphaFold structure (p-value = 0.010). The logAUC based on idock for DUD-E structure was 0.252 ± 0.113 while 0.228 ± 0.088 for AlphaFold structure (p-value = 0.021). Notably, the virtual screening based on autodock4 scoring function yielded better results on all metrics. The results suggest that the protein structure in DUD-E database was slightly better than AlphaFold predicted structure for virtual screening. The selection of scoring functions had a great impact on the results of virtual screening (Table 1). The results for autodock4, idock, rf_score and vinardo based on DUD-E structures and AlphaFold structures of every target are shown in Supplementary Information Table 2-9.

Virtual screening results of Holo, AlphaFold and Apo protein structures

Previous studies have shown that the virtual screening result of Holo structure is generally better than that of Apo structure. The protein structure in the DUD-E database is Holo structure. To evaluate whether AlphaFold protein structure produces better result compared to Apo structure in virtual screening, we tried to collect the Apo structure for the 51 selected targets in DUD-E database. However, only 23 out of these 51 targets have Apo structure available in the PDB database with known binding pocket. We then performed virtual screening with the Apo structures of these 23 targets.

Molecular docking is a technique that involves fitting small molecules into the binding pocket of a protein structure and allows for the identification of appropriate conformations. Therefore, the binding pocket is essential for virtual screening using molecular docking. When analyzing the protein structures, we found that HIVRT has clear binding pocket in its Holo and Apo structures encompassing the small co-crystalline molecules. However, no apparent binding pocket was found in its AlphaFold structure (Fig. 2a), so HIVRT was not included in the 23 targets mentioned above. On the other hand, AKT2, has clear binding pockets in its Holo and AlphaFold structures but not in the Apo structure (Fig. 2b). Therefore, AKT2 was also excluded from the selected targets.

The AUC values between Holo and Apo groups were significantly different when using scoring function autodock4 (Holo 0.628 ± 0.154, Apo 0.580 ± 0.142, p-value = 0.040), idock (Holo 0.641 ± 0.152, Apo 0.603 ± 0.144, p-value = 0.043). With the vinardo function, AlphaFold structures were significantly better than Apo structures in terms of EF1% (AlphaFold 4.183 ± 4.919, Apo 2.311 ± 2.455, p-value = 0.032) and logAUC (AlphaFold 0.230 ± 0.087, Apo 0.210 ± 0.074, p-value = 0.042). It shows that the protein structure in DUD-E database is better than Apo structure in virtual screening. The protein structure in DUD-E database is slightly better than AlphaFold protein structure for virtual screening, and AlphaFold protein structure is slightly better than Apo protein structure in virtual screening.

It is worth noting that the difference between DUD-E and AlphaFold groups in Figure 2c is relatively smaller than the difference in Figure 1c. It is because the number of protein targets tested in Figure 2c is less. The virtual screening of protein structure in DUD-E database (the average of logAUC for idock is 0.244) was better than the average value of AlphaFold protein structure (the average of logAUC for idock is 0.220) in different scoring functions and different indicators. And the virtual screening of AlphaFold protein structure is better than the overall scores of protein Apo structure (the average of logAUC for idock is 0.202), while different scoring functions have a significant impact on the results of virtual screening (Table 2). The

results for autodock4, idock, rf_score and vinardo based on Apo structures of every target are shown in Supplementary Information Table 10-13.

Evaluation of consensus scoring method based on score or ranking

Previous studies have shown that consensus scoring based on multiple scoring functions[20–23] can take advantages of each scoring function to achieve better screening results. However, different scoring functions may need to be standardized before they can be integrated. Common standardization methods include ranking, AASS, Average of auto scaled scores, Z-score scaling.

In this study, we selected four appropriate scoring functions (autodock4, idock, rf_score, and vinardo) and combined them using 12 different consensus scoring methods (3 standardization methods × 4 consensus calculation methods). We tested these methods on 51 previously selected targets, with the results of the four single scoring functions as controls.

Different scoring functions may produce similar results, which will not help improving the consensus outcome. So, we tested the correlation between each one another among the five scoring functions including autodock4, idock, qvina, rf_score and vinardo. The correlation coefficient R^2 between qvina and idock is greater than 0.9 (for logAUC is 0.937, for BEDROC(α=80.5) is 0.930) and the fitting line (for logAUC is $y = 0.909x + 0.018$, for BEDROC(α=80.5) is $y = 1.058x + 0.002$) is close to y=x (Fig. 3a), while the correlation coefficient R^2 between other pairs are less than 0.75. These results indicated that qvina and idock have a high similarity. In fact, qvina and idock are both developed based on AutoDock Vina. Therefore, we finally selected autodock4, idock, rf_score and vinardo scoring functions for consensus scoring.

To show four different calculation methods of consensus scores, we compared the distribution score of idock, rf_score and consensus evaluation methods on the representative BACE1 protein (Fig. 3b). From the distribution of active compounds and decoy compounds, the top small molecules were more likely to be active

compounds (for idock the EF10% is 2.66 while for rf_score the EF10% is 2.87), indicating that idock and rf_score has certain ability to enrich active compounds. Moreover, we found that the best exp_z_score, consensus score of exponential function based on Z-score scaling, was generally better than that of autodock4, idock and rf_score and vinardo scoring functions. The exp_z_score were also superior to most other consensus scoring methods (Fig. 3c).

The exp_rank (ECR) was also a consensus scoring method based on ranking exponential function. Compared the consensus score of ECR and exp_z_score groups by paired t-test, exp_z_score showed better than ECR method (for example, logAUC for exp_z_score is 0.290 while for ECR is 0.284), except for the AUC (for exp_z_score is 0.686 while for ECR is 0.689). Notely, BEDROC(α=20.0) and EF10% of exp_z_score (0.253 and 3.202) are higher than that of ECR (0.244 and 3.104) with significant difference (p-value is 0.028 and 0.028)(Table 3). The results for scoring function and consensus scoring function (including using 4, 3, 2 scoring functions) based on DUD-E structures, AlphaFold structures and Apo structures are shown in Supplementary Information Table 14-16.

Re-evaluation of Holo, AlphaFold and Apo protein structures using consensus scoring method

We also evaluated the virtual screening results of Holo, AlphaFold and Apo protein structures with four representative consensus scores. Again, with the consensus scoring functions, DUD-E structure generated better results compared to AlphaFold protein structure (such as for exp_z_score, the logAUC for DUD-E is 0.290 ± 0.133 while the logAUC for AlphaFold is 0.256 ± 0.096, and the p-value for logAUC between DUD-E and AlphaFold is 0.014)(Fig. 4a). The average values of main data groups have substantial differences, while the direct average values of a few data groups do not have significant differences. Remarkably, AlphaFold structure is slightly better than Apo structure in virtual screening with the consensus scores (such as for exp_z_score, the EF1% for AlphaFold is 5.161 ± 5.284 while the EF1%

for Apo is 3.223 ± 5.321, and the p-value for EF1% between AlphaFold and Apo is 0.050)(Fig. 4b).

In addition, for each of the 51 previously selected targets, we also made a difference in each index of the AlphaFold protein structure and protein Holo structure screening results, namely AlphaFold – DUD-E (Fig. 4c). If the difference of defined logAUC is less than -0.03, it indicates that the virtual screening result of AlphaFold protein structure is worse than that of DUD-E protein structure. If the difference of defined logAUC is greater than or equal to -0.03 and less than or equal to 0.03, it indicates that the virtual screening result of AlphaFold protein structure is equivalent to that of DUD-E protein structure. If the difference of defined logAUC is greater than 0.03, it indicates that the virtual screening result of AlphaFold protein structure is better than that of DUD-E protein structure. There are 20 targets (about 39%) with AlphaFold protein structure worse than DUD-E protein structure, 18 targets (about 35%) with AlphaFold protein structure equivalent to DUD-E protein structure, and 13 targets (about 25%) with AlphaFold protein structure better than DUD-E protein structure.

We also studied the 51 protein Holo structure and AlphaFold protein structure for exp_z_score by paired t-test. The average AlphaFold minus DUD-E of all indicators were negative value, and there is a significant difference between the average AlphaFold and DUD-E of most indicators (Table 4). These similar results were also observed in the situation of that of Apo minus AlphaFold (Table 5). With consensus scoring of virtual screening, Holo protein structures from DUD-E database were better than AlphaFold protein structure, which were better than Apo structures. The results for exp_z_score consensus scoring function based on DUD-E structures, AlphaFold structures and Apo structures of every target are shown in Supplementary Information Table 17-19.

Multi-stage screening combined with consensus scoring

Although the virtual screening effect of the best consensus scoring obtained in the test is better than that of a single scoring function, consensus scoring is based on multiple scoring functions. The computing resources consumed in the whole process of consensus scoring are the sum of all the computing resources consumed by the involved single scoring function and docking software, which consumes more computing resources.

With the rapid expansion of the small molecule compound library that can be used for virtual screening, large-scale virtual screening is also increasingly widely used. Therefore, it is of great significance to improve the efficiency of virtual screening and reduce the computing resources consumed by virtual screening to save the cost of large-scale virtual screening and accelerate the drug screening process. Several studies have used multi-stage screening to improve the efficiency of virtual screening. Multi-stage screening uses rough but fast screening in the first part of the stage, and more refined but slow screening in the second part of the stage, so as to give consideration to the early enrichment ability and computational efficiency of virtual screening.

In order to use the advantages of consensus scoring to improve the ability of virtual screening and reduce the computational resources consumed in the whole process of consensus scoring, we propose a multi-stage screening combined with consensus scoring (Fig. 5a).It is worth noting that since our study above has performed virtual screening on 51 targets, and the scores of different scoring functions between all proteins and small molecules are known, multi-stage screening (plan A, B, C, D, E, F) does not actually perform virtual screening, but uses corresponding known data, and the time consumed is also a theoretical estimate calculated based on known data.

On the crucial EF1% index for evaluating the early enrichment ability of virtual screening, the multi-stage screening plan A, C and E maintain a relatively high score (the average value of EF1% for plan A is 7.80, for plan C is 7.68, for plan E is 7.55) in comparison with the exp_z_score method (the average value of EF1% is 7.74, the p-value for EF1% between plan E and exp_z_score is 0.420). With the reduction of the

consumed time for the multi-stage screening scheme, EF1% had a slight downward trend, but still can keep a higher value. In addition, the EF1% of multi-stage screening with using consensus scoring (for plan E is 7.55) is higher than that without consensus scoring (for plan F is 6.62) (Fig. 5b and Table 6). These indicated that the multi-stage screening using consensus score would remarkably improve the virtual screening results.

BEDROC is an important indicator of early enrichment capacity (α=80.5). We also observed that multi-stage screening plan A, C and E with consensus scoring (the average value of BEDROC(α=80.5) for plan A is 0.203, for plan C is 0.197, for plan E is 0.189) exhibited a higher score of BEDROC relative to exp_z_score (the average value of BEDROC(α=80.5) is 0.204, the p-value for BEDROC(α=80.5) between plan E and exp_z_score is 0.032)(Fig. 5c), but a worse score in terms of AUC (the average value of AUC for plan A is 0.666, for plan C is 0.659, for plan E is 0.657, for exp_z_score is 0.686. The p-value for AUC between plan E and exp_z_score is 0.0005) and logAUC (the average value of logAUC for plan A is 0.276, for plan C is 0.268, for plan E is 0.262, for exp_z_score is 0.290. The p-value for AUC between plan E and exp_z_score is 0.0002) indicators. These results demonstrated that multi-stage screening combined with consensus score had a great advantage in early enrichment ability which is of great significance for drug discovery.

There was no significant difference between Plan E and exp_z_score in the term of EF1% values (p=0.420), while the average calculation speed of each small molecule of Plan E (7.04 second/cpu/molecule) is nearly 9 times faster than exp_z_score (63.51 second/cpu/molecule). Therefore, multi-stage screening combined with consensus scoring can use the advantages of consensus scoring to synthesize each single scoring function to improve the ability of virtual screening effect, while significantly reducing the computational resources consumed in the whole process of consensus scoring. The multi-stage screening combined with consensus score has higher early enrichment ability and less computational resource consumption, which is of great significance for large-scale drug screening.

Relationship between scoring score and hit rate

In addition, we also analyzed four single scoring functions exp_z_score function of 51 protein targets from both DUD-E protein structures and AlphaFold protein structures, and counted their distributions and hit rates of small molecules.

To understand the relationship between the scoring and hit rate of small molecules in various scoring methods, we calculated the hit rate of active small molecules in the corresponding score segment of each scoring method. We found that the smaller the score of the autodock4, idock, and vinardo scoring functions, the more likely the small molecule is to combine with the protein. Moreover, as the score decreases, the hit rate tends to increase (Fig. 6a, b, e, f, i, j blue and green curves). While, according to the core algorithms of rf_score and exp_z_score functions, the higher values demonstrated that these small molecules were more likely to combine with the protein. With the increase of the score, the hit rate tends to increase in terms of rf_score and exp_z_score (Fig. 6c, d, g, h blue and green curves). For different methods, small molecule compounds with better scores are more likely to be active small molecule compounds and deserve more attention. This is also one of the bases for multi-stage screening to select the top small molecules for further screening in the next stage.

Since the number of molecules in some fraction segments of higher and lower scores is small, the hit rate error corresponding to the fraction segment may be large. So there is some fluctuation on the curve. The curve of score and hit rate is of great significance for evaluating the scores given by different methods. It is helpful for researchers to set threshold values based on scores and give priority to small molecules that are more likely to be active compounds. For example, if the score of a small molecule on a protein is less than -9 by using the autodock4 scoring function for docking, the small molecule is more likely to be an active small molecule.

Discussion

We used the targets in the DUD-E database, which is widely used in the benchmark test of virtual screening, and selected their corresponding AlphaFold structure and protein Apo structure. We applied a variety of docking software, multiple scoring functions and consensus scoring methods to perform virtual screening. To evaluate AlphaFold protein structure for virtual screening, we compared the performance of the protein structure of AlphaFold protein and DUD-E database, which represents the protein Holo structure.

We found that in the test of 51 selected targets, the virtual screening effect of protein structure in DUD-E database is better than that of AlphaFold protein structure as a whole, but there are 18 targets (about 35%) whose AlphaFold protein structure is equivalent to that of DUD-E protein, and 13 targets (about 25%) whose AlphaFold protein structure is better than that of DUD-E. In the test of 23 selected targets, it was found that the virtual screening effect of protein structure in DUD-E database was slightly better than that of AlphaFold protein structure, and AlphaFold protein structure was slightly better than that of Apo protein structure. Our results have guiding significance for the selection of protein structures in virtual screening. Generally, when the protein Holo structure is available, the protein Holo structure is preferred. When the protein Holo structure is not available, the AlphaFold protein structure can be used preferentially.

At present, the AlphaFold protein structure database has more than 200 million entries, providing human proteome and proteome of 47 other organisms. Although AlphaFold is only used to predict the monomer protein structure, it can be used to predict the protein composed of multiple monomers[29]. In addition, you can also use ColabFolder[30], which is more user-friendly and easy to use, instead of installing the AlphaFold program and downloading the required database locally. Combined with our conclusions, the super large-scale protein structure database and low-cost and fast accurate method from sequence to three-dimensional protein structure provided by AlphaFold are of excellent use value for virtual screening, and of great significance for speeding up drug discovery and reducing drug development costs.

We tested 13 consensus scoring methods and found the exp_z_score was generally better than other methods, which showed to be higher than ECR in terms of BEDROC (α= 20.0) and EF10%. The advantage of exp_z_score consensus method may be that it used a more reasonable Z-score standardized method and exponential function that was more regular for virtual screening. The Z-score standardization method can standardize the scoring data group of the scoring function for the small molecule set to the data group with a mean value of 0 and a standard deviation of 1. Compared with the standardized method of Rank, the Z-score standardization method can better retain the difference information of the same scoring function for different small molecules. In addition, the Z-score standardization method is less affected by the maximum and minimum values than the AASS standardization method.

With the rapid expansion of the small molecule compound library available for virtual screening and the super extensive protein structure database provided by AlphaFold, the large-scale virtual screening will play an increasingly important role in drug discovery. To reduce the computing time of virtual screening, improve the computing efficiency, save computing resources, and be able to use a variety of different scoring functions and consensus scoring methods, we propose a multi-stage screening combining consensus scoring methods. The average value of EF1% has no significant difference compared with consensus scoring, but its speed is about 9 times that of consensus scoring. Multi-stage screening combined with consensus score can flexibly adjust the number of small molecules screened at each stage to adjust the time and screening effect. It only uses a small amount of computing resources and has a high early enrichment capacity. Compared with the traditional multi-stage screening, the multi-stage screening combined with consensus score has great advantages in the early enrichment ability. Multi-stage screening combined with consensus score is used for large-scale drug screening, which is of great significance for speeding up drug discovery and reducing drug development costs.

We tried to optimize the AlphaFold structure by molecular dynamics inorder to improve the virtual screening. This seems like a potential approach from the results of wee1 target shown in the Supplementary Information Table 20. But we can’t split the

good structures from other structures for virtual screening without the active and decoy label. In other words, we can't split the good structures from other structures by some simple indication such as the best score or the average score. Our results and conclusions are similar to Nichols et al. In their studies they found that molecular dynamics can improve virtual screening results but they can't identify any evident relationship between characterization of molecular dynamics snapshots and virtual screening results[31].

In the process of determining the structure of the protein used, we found that some proteins, such as HIVRT, had apparent binding pocket structures in their Holo and Apo structures around the positions of small co-crystalline molecules. But there was no obvious binding pocket structure in the AlphaFold protein structure. However, some proteins, such as AKT2, had obvious binding pocket structures in the Holo structure and AlphaFold structure around the eutectic small molecules, but there was no obvious binding pocket structure in the Apo structure. This indicated the typical inductive fit effect between proteins and small molecules. However, among the targets we examined, most AlphaFold protein structures and Apo protein structures have obvious binding pocket structures, which may be related to the flexibility of amino acid residues from protein binding pocket. These results also suggested the limitation of AlphaFold's prediction of protein structure: it was difficult to fully consider the impact of non-protein parts on protein structure, and it was unable to give non-protein structures such as water molecules, coenzymes, metal ions, etc. Since AlphaFold did not give a non-protein structure, we have removed the non-protein structure part from all tested protein structures.

We use AutoSite[32] to determine the search space, which has the advantage that we can flexibly describe the binding pocket structure of proteins. However, the multiple binding site structures given by AutoSite still need to be selected according to the position of small co-crystalline molecules relative to the protein structure. In addition, the combination pocket structure provided by AutoSite may be too large or too small. To avoid the influence of human operation on the experimental results, we

did not adjust the search space separately when the combined bag structure was too large or too small.

For our research, there are still some limitations. The number of targets used to compare protein Holo structure and AlphaFold structure is 51, and the number of targets used to compare protein Holo structure, protein Apo structure and AlphaFold structure is 23. Although some valuable data have been obtained from these targets, more targets can be used for testing to obtain more reliable data. In the treatment before the virtual screening of protein Holo structure, protein Apo structure and AlphaFold structure, we removed the non-protein structural parts from all structures. In the practical application of virtual screening, the non-protein components in protein Holo structure and protein Apo structure, such as water molecules, coenzymes, and metal ions, may be considered. The docking used in the study regards protein structure as rigid, while small molecules as flexible. Therefore, flexible docking[33], that is, the amino acid residues in protein binding pockets are considered flexible and small molecules are considered flexible, which may be a method worth trying. The limitation of the curve drawn based on the relationship between scoring and hit rate lies in the high proportion of active small molecules in the DUD-E database and the small number of small molecules in the small molecule set, which is quite different from the large-scale virtual screening. In the test of consensus scoring method, we only considered the scoring of small molecules by the scoring function of docking software, but did not consider docking conformation. Taking into account docking conformation for consensus scoring may be a method worth trying. In the multi-stage screening test, the number of stages divided is three, and only three groups of schemes are set according to the proportion of small molecules entering the next stage in each stage. What's more, the small molecule set used for testing has fewer small molecules, which is several orders of magnitude less than the small molecule library of super large-scale virtual screening. Therefore, although our research can provide some guidance for super large-scale virtual screening, it is difficult to give a specific implementation plan for large-scale virtual screening. Further work is needed to develop a specific implementation plan for large-scale virtual screening.

Methods

Targets

To evaluate the effectiveness of AlphaFold protein structure in virtual screening, we used the targets in the DUD-E database. The DUD-E database contains 102 protein targets, each of which includes protein structure (from the PDB database), co-crystalline small molecules to determine the docking software search space, active small molecules and decoy small molecules. It is widely utilized to assess the ability of virtual screening to distinguish active compounds from decoy compounds.

To ensure the diversity of protein types and the binding site of targets, we selected 51 representative targets in the DUD-E database as our test targets representing eight types of protein targets namely protease, nuclear receiver, kinase, cytochrome P450, ion channel, GPCR, other enzymes and miscellaneous proteins (Fig. 1a). In total, more than 400,000 small molecules which interact with these 51 targets were used.

We tried to collect the Apo structure for the 51 selected targets in DUD-E database. However, only 23 out of these 51 targets have Apo structure available in the PDB database with known binding pocket. The information including the PDB ID and the resolution of 23 Apo structures can be find in the Supplementary Information Table 1.

ColabFold

Milot Mira et al. developed ColabFold based on Google Colab in order to enable researchers without relevant hardware resources to use AlphaFold2[30].

Because HIVPR and HIVRT are non-monomer proteins, their protein structures cannot be directly obtained in the AlphaFold Database, so ColabFold is used for structure prediction.The input sequence and configuration can be find in the Supplementary Information.

Protein structure preparation

Considering the calculation time of virtual screening, the diversity of protein types and whether the AlphaFold protein structure can be used for virtual screening (structure availability and whether there is an obvious binding site), the DUD-E Database is selected(http://dude.docking.org/targets)to 51 targets in are used as virtual screening test targets.

The protein structure provided by DUD-E database corresponding to the 51 selected targets is used as the test target of protein Holo structure. There are 50 AlphaFold protein structures corresponding to 51 targets from AlphaFold Database(https://alphafold.com/). HIVPR protein is predicted by ColabFold. The AlphaFold protein structure corresponding to all 51 targets serves as the virtual screening test target.

Because some proteins cannot or are difficult to find their Apo structures in the PDB database, and some proteins have no apparent binding sites, only 23 of the 51 targets found available protein Apo structures as virtual screening test targets.

Each protein structure that is the target of the virtual screening test is processed as follows:

1. Use PDBFixer 1.8.1(https://github.com/openmm/pdbfixer), replace non-standard residues, remove heterologous substances (including water molecules, coenzymes, metal ions, etc.), and add missing atoms to obtain the acceptor_ fixed.pdb.

2. Use the script provided by AutoDock Vina to execute the following commands:

prepare_ receptor -r receptor_ fixed. pdb -o receptor. pdbqt -A hydrogens

The final receiver Pdbqt is the prepared protein file, which can be directly used as the input of AutoDock Vina, Qvina2 and idock to perform docking.

Compounds preparation

We get the active small molecule files corresponding to each target from DUD-E Database_ final.sdf.gz and decoy small molecule file decoys_ final.sdf.gz. Next, decompress and use openbabel 3.1.0[34] (https://github.com/openbabel/openbabel), perform split conversion to obtain the mol2 format file corresponding to each small molecule, and then use the script provided by AutoDock Vina for each small molecule

to execute the following commands for hydrogenation and preparation of small molecule file formats:

prepare_ ligand -l molecule. mol2 -o molecule. pdbqt -A hydrogens

The final obtained Molecule Pdbqt is the prepared small molecule file, which can be directly used as the input of AutoDock Vina, Qvina2 and idock to perform docking.

Search space

AutoSite 1.0.0[32] is used to predict binding sites for each protein structure that is the target of the virtual screening test, and PyMOL (TM) Molecular Graphics System, Version 2.6.0a0 Open-Source[35] is used to visually inspect and select binding sites.

For the protein structure in the DUD-E database, refer to the eutectic small molecule crystal in the DUD-E database_ The position of ligand.mol2 selects the binding site.

For the AlphaFold protein structure and Apo structure, align the protein structure and small co-crystalline molecules corresponding to the target in the DUD-E database with the AlphaFold protein structure and Apo structure. Then, select the binding site by referring to the position of small co-crystalline molecules.

After determining the protein structure binding site, use the PandasPdb module of biopandas 0.2.9 to calculate the spatial coordinate information of the binding site structure, including size and location, and then add 8 Å to each of the x, y, and z dimensions of the binding site structure size as the search space for AutoDock Vina, Qvina2, and idock.

Docking

Three docking software AutoDock Vina 1.2.3, QuickVina 2.1 (Qvina2) and idock 2.2.3 are used. And five scoring functions including autodock4 and vinardo in AutoDock Vina, qvina scoring function, idock scoring function, and rf_scoring function in idock were employed. For each docking, the seed used is 20011204, and only the best docking position is considered as output. The exhaustiveness value used

by AutoDock Vina and Qvina2 is 1, and the tasks used by idock are 8. Neither flexible docking nor hydration docking is used.

The used autodock4 (ad4) scoring function and vinardo scoring function are the scoring functions provided by AutoDock Vina 1.2.3. When using the autodock4 scoring function and vinardo scoring function, perform docking respectively to obtain the scoring of a single small molecule by autodock4 scoring function and the scoring of a single small molecule by vinardo scoring function. Affinity map is also required when using the autodock4 scoring function. Each docking is prepared by autogrid4 (AutoGrid 4.2.7. x.2019-07-11) and AutoDock Vina_ The affinity graph was calculated by gpf.py.

The qvina scoring function used is QuickVina 2.1 scoring function.

The score function used by idock and rf_score is provided by idock 2.2.3. When idock 2.2.3 is executed, only one time of docking would be performed to obtain the score of idock and rf_score functions for a single small molecule screening.

Consensus scoring

For every target, to integrate different scoring functions, different scoring functions may need to be standardized. Common standardization methods include Rank, AASS(Average of auto-scaled scores), Z-score, etc. Only after the scores between different scoring functions are standardized can they be reasonably calculated and compared.

According to the direction of scoring, the scoring function can be divided into two categories. The first category is that the larger the scoring value represents the stronger the binding ability of small molecule compounds to protein. The second category is that the higher the score represents the weaker the binding ability of small molecule compounds to proteins is.

The effective scores of the first category are all scores with a score value greater than 0; The second type of valid score is all scores with a score value less than 0.

Rank

Rank as the standardized score.

For the first category, the scores are sorted from the largest to the smallest.

For the second category, the scores are sorted from the smallest to the largest.

That is, the scores from two categories are ranked from good to bad. And then, use rank as standardized score for the tow categories. The smaller the standardized score, the better.

Z-score

Standardize score S_{ij} for small molecule j on scoring function i by Z-score to obtain the standardized score Z_{ij}。

The mean of the effective scores on the scoring function i is $\overline{S_i}$, and the standard deviation of that is σ_i.

The scores from the first category are standardized by the following formula:

$$Z_{ij} = \frac{S_{ij} - \overline{S_i}}{\sigma_i}$$

The scores from the second category are standardized by the following formula:

$$Z_{ij} = \frac{\overline{S_i} - S_{ij}}{\sigma_i}$$

For the two categories, the larger the standardized score, the better.

AASS

Standardize score S_{ij} for small molecule j on scoring function i by AASS to obtain the standardized score A_{ij}.

For the first category and the scoring function i, the largest score is $Best_i$, the smallest score is $Worst_i$.

For the second category and the scoring function i, the smallest score is $Best_i$, the largest score is $Worst_i$.

That is, for the two categories, the best score is $Best_i$, the worst is $Worst_i$.

The scores from the two categories are standardized by the following formula:

$$A_{ij} = \frac{S_{ij} - Worst_i}{Best_i - Worst_i}$$

For the two categories, the larger the standardized score, the better.

At the same time, another key to consensus scoring is how to process standardized scores to obtain the final consensus score.

We selected four calculation methods: Summation (Sum), Best, Worst, and Summation after Exponentiation (Exp).

Sum

The standardized score for small molecule j on scoring function i is V_{ij}. The consensus score Sum_j for small molecule j is calculated by the following formula:

$$Sum_j = \sum_i V_{ij}$$

Best

The consensus score $Best_j$ for small molecule j is the best standardized score in every scoring function.

Worst

The consensus score $Worst_j$ for small molecule j is the worst standardized score in every scoring function.

Exp

The standardized score for small molecule j on scoring function i is V_{ij}. The consensus score Exp_j for small molecule j is calculated by the following formula:

$$Exp_j = \sum_i e^{V_{ij}}$$

Consensus function

According to the combination of standardization methods (3) and calculation methods (4), 12 consensus scoring methods were obtained. The combination and name are as follows:

	Rank	Z-score	AASS
Sum	sum_rank	sum_z_score	sum_aass
Best	best_rank	best_z_score	best_aass
Worst	worst_rank	worst_z_score	worst_aass
Exp	exp_rank	exp_z_score	exp_aass

For example, the complete description of exp_z_score is as follows:

The mean of the effective scores on the scoring function i is $\overline{S_i}$, and the standard deviation of that is σ_i. The standardized score for small molecule j on scoring function i is Z_{ij}.

The scores from the first category are standardized by the following formula:

$$Z_{ij} = \frac{S_{ij} - \overline{S_i}}{\sigma_i}$$

The scores from the second category are standardized by the following formula:

$$Z_{ij} = \frac{\overline{S_i} - S_{ij}}{\sigma_i}$$

The final consensus score Exp_j for small molecule j is calculated by the following formula:

$$Exp_j = \sum_i e^{Z_{ij}}$$

The larger the final consensus score, the more likely it is an active small molecule.

While exp_rank(ECR) has changed the method of Exp:The rank for small molecule j on scoring function i is R_{ij}. The number of the effective scores on the scoring function i is n_i. The consensus score Exp_j for small molecule j is calculated by the following formula:

$$Exp_j = \sum_i e^{-R_{ij}/(n_i * 10\%)}$$

The larger the final consensus score, the more likely it is an active small molecule.

In addition, Rank by Vote (RBV) consensus scoring method was tested.

RBV

The threshold value is set to x=top10% and the ranking of small molecule j in the scoring function i is within the threshold value x, one vote will be obtained. The sum of votes of small molecule j on all scoring functions is the final score. Small molecules with the same number of votes are randomly ranked.

Multi-stage virtual screening with consensus ranking

Prepare small molecules, proteins and search space, and then start multi-stage screening. In the first stage, idock docking is used for virtual screening to obtain idock rank and rf_score rank, and then ir rank is obtained through the consensus score of idock rank and rf_score rank. The top x% of the ir rank are taken to enter the second stage. In the second stage, we use the vinardo scoring function to conduct virtual screening to obtain the vinardo rank, and then take the small molecules in the topx% of the ir rank in the idock rank and rf_score rank and all the small molecules in the vinardo rank for consensus scoring to obtain the irv rank. The top y% of the irv rank are taken to enter the third stage. In the third stage, the autodock4 scoring function is used to conduct virtual screening, and the autodock4 rank is obtained. Then the small molecules in idock rank, rf_score rank and vinardo rank that are y% before irv rank and all small molecules in autodock4 rank are scored by consensus to obtain irva rank. The final ranking is obtained by ranking the small molecules in irva rank, the small molecules in irv rank that are not in irva rank, and the small molecules in irv rank that are not in irv rank according to the original order within the ranking. The x and y parameters can be adjusted flexibly. Three groups of schemes are set, Plan A(x=40，y=50)，Plan C(x=20，y=50)，Plan E(x=10，y=50).

Multi-stage virtual screening without consensus ranking

Prepare small molecules, proteins and search space, and then start multi-stage screening. In the first stage, idock docking is used for virtual screening to obtain idock rank, the top x% of the idock rank are taken to enter the second stage. In the second stage, we use the vinardo scoring function to conduct virtual screening to obtain the vinardo rank, the top y% of the vinardo rank are taken to enter the third stage. In the third stage, the autodock4 scoring function is used to conduct virtual screening, and the autodock4 rank is obtained. The final ranking is obtained by ranking the small molecules in autodock4 rank, the small molecules in vinardo rank that are not in autodock4 rank, and the small molecules in idock rank that are not in vinardo rank according to the original order within the ranking. The x and y parameters can be

adjusted flexibly. Three groups of schemes are set, Plan B(x=40 , y=50) , Plan D(x=20 , y=50) , Plan F(x=10 , y=50).

Metrics

We used AUC (area under the receiver operating characteristic curve), logAUC (area under the semilogarithmic receiver operating characteristic curve), EF1% (enrichment factor 1%), EF5%, EF10% and BEDROC (Boltzmann-enhanced discrimination of receiver operating characteristic, α= 321.9, α= 80.5, α= 20.0) as benchmark metrics to assess the result. LogAUC is the area under the semi-logarithmic ROC curve, and the early enrichment capacity has a greater weight in logAUC than AUC[12] . Enrichment factors (1%, 5%, and 10%) are used to truncate the assessment of early enrichment capacity under specific thresholds, which are closely related to the practical application of virtual screening. The BEDROC[36] was proposed to consider all small molecules by adjusting α value for the weight of early enrichment capacity. The greater the early enrichment capacity, the larger α weight value.

Hits rate

In a collection of small molecules, the number of active compounds in the collection is $actives$, the number of all compounds in the collection is $total$. $Hits\ rate$ is calculated by the following formula:

$$Hits\ rate = \frac{actives}{total}$$

For a collection of small molecules in the top x% of a rank, the number of active compounds in the collection is $actives(x\%)$, the number of all compounds in the collection is $total(x\%)$. $Hits\ rate(x\%)$ is calculated by the following formula:

$$Hits\ rate(x\%) = \frac{actives(x\%)}{total(x\%)}$$

Enrichment factor

For a collection of small molecules in the top x% of a rank, the enrichment factor x%(EFx%) is calculated by the following formula:

$$EFx\% = \frac{Hits\ rate(x\%)}{Hits\ rate(100\%)}$$

BEDROC

BEDROC is defined as follows:

$$BEDROC(\alpha) = \frac{\sum_{i=1}^{n} e^{-\alpha r_i/N}}{\frac{n}{N}\left(\frac{1-e^{-\alpha}}{e^{\alpha/N}-1}\right)} \times \frac{R_a \sinh(\alpha/2)}{\cosh(\alpha/2) - \cosh(\alpha/2 - \alpha R_a)} + \frac{1}{1-e^{\alpha(1-R_a)}}$$

While the n is the number of active compounds, the N is the number of all compounds, the rate $Ra = n/N$, the r_i is the rank of i th active compound[36].

Receiver Operating Characteristics (ROC) Curve and its area under the curve (AUC)

The Y-axis is the true positive rate (TPR, also named actives found rate)under a specific threshold. The X-axis is the false positive rate (FPR, also named decoys found rate)under a specific threshold.

TPR is calculated by the following formula:

$$TPR = \frac{TP}{TP + FN}$$

FPR is calculated by the following formula:

$$FPR = \frac{FP}{FP + TN}$$

At a specific threshold, TP is the number of true positive compounds, FN is the number of false negative compounds, FP is the number of false positive compounds, and TN is the number of true negative compounds.

The area under the ROC curve is AUC, and its value range is [0,1]. The AUC corresponding to random screening is 0.5.

Semilogarithmic Receiver Operating Characteristics (ROC) Curve and its area under the curve (logAUC)

After drawing ROC curve, let λ= 0.001. Points with abscissa less than λ are ignored and the abscissa of other points is performed logarithmic(log_{10}) operation. That is, the point (x_i, y_i) in the ROC curve, the point $(log_{10}(x_i), y_i)$ in the semilogarithmic ROC.

The abscissa value range of Semilogarithmic ROC curve is [-3,0]. The area of semilogarithmic ROC curve is $area$. Let $logAUC = area/3$, and its value range is [0,1].

Time

Use the Linux time command to count the time, and use user time+sys time as the time used for virtual screening.

System

All docking calculations are performed in containers created by images built with Docker 20.10.17 software. Docker is an open source lightweight virtualization technology (https://www.docker.com/).

The host system is Linux 5.4.0-131 generic.

CPU

Intel(R) Xeon(R) Gold 6238R CPU @ 2.20GHz.

Figure

Violin chart, ROC curve, scatter plot, fitting line and histogram are drawn with matplotlib 3.6.1[37].

The three-dimensional structure diagram of small molecules and protein is drawn with PyMOL (TM) Molecular Graphics System, Version 2.6.0a0 Open-Source[35].

Funding

This work was supported by National Natural Science Foundation of China (82260488 and 32200679), China Postdoctoral Science Foundation (2021TQ0137, 2021M701544), Yunnan Applied Basic Research Key Projects (202001AT070102, and 202001AT070104), Natural Science Foundation of Chongqing (CSTB2022NSCQ-MSX056), Postgraduate innovation special fund project of Jiangxi (YC2022—s047), College Students' Innovative Entrepreneurial Training Plan Program of Nanchang University (2022CX024, 2022CX158), Scientific Research Training Program of Nanchang University (2022).

Conflict of interest

The authors declare that they have no conflict of interest.

Reference

(1) Jumper, J.; Evans, R.; Pritzel, A.; Green, T.; Figurnov, M.; Ronneberger, O.;

Tunyasuvunakool, K.; Bates, R.; Žídek, A.; Potapenko, A.; Bridgland, A.; Meyer, C.; Kohl, S. A. A.; Ballard, A. J.; Cowie, A.; Romera-Paredes, B.; Nikolov, S.; Jain, R.; Adler, J.; Back, T.; Petersen, S.; Reiman, D.; Clancy, E.; Zielinski, M.; Steinegger, M.; Pacholska, M.; Berghammer, T.; Bodenstein, S.; Silver, D.; Vinyals, O.; Senior, A. W.; Kavukcuoglu, K.; Kohli, P.; Hassabis, D. Highly Accurate Protein Structure Prediction with AlphaFold. *Nature* **2021**, *596* (7873), 583–589. https://doi.org/10.1038/s41586-021-03819-2.

(2) Binder, J. L.; Berendzen, J.; Stevens, A. O.; He, Y.; Wang, J.; Dokholyan, N. V.; Oprea, T. I. AlphaFold Illuminates Half of the Dark Human Proteins. *Current Opinion in Structural Biology* **2022**, *74*, 102372. https://doi.org/10.1016/j.sbi.2022.102372.

(3) Ros-Lucas, A.; Martinez-Peinado, N.; Bastida, J.; Gascón, J.; Alonso-Padilla, J. The Use of AlphaFold for In Silico Exploration of Drug Targets in the Parasite Trypanosoma Cruzi. *Frontiers in Cellular and Infection Microbiology* **2022**, *12*.

(4) Weng, Y.; Pan, C.; Shen, Z.; Chen, S.; Xu, L.; Dong, X.; Chen, J. Identification of Potential WSB1 Inhibitors by AlphaFold Modeling, Virtual Screening, and Molecular Dynamics Simulation Studies. *Evidence-Based Complementary and Alternative Medicine* **2022**, *2022*, e4629392. https://doi.org/10.1155/2022/4629392.

(5) Yang, C.; Alam, A.; Alhumaydhi, F. A.; Khan, M. S.; Alsagaby, S. A.; Al Abdulmonem, W.; Hassan, M. I.; Shamsi, A.; Bano, B.; Yadav, D. K. Bioactive Phytoconstituents as Potent Inhibitors of Tyrosine-Protein Kinase Yes (YES1): Implications in Anticancer Therapeutics. *Molecules* **2022**, *27* (10), 3060. https://doi.org/10.3390/molecules27103060.

(6) Wong, F.; Krishnan, A.; Zheng, E. J.; Stärk, H.; Manson, A. L.; Earl, A. M.; Jaakkola, T.; Collins, J. J. Benchmarking AlphaFold-Enabled Molecular Docking Predictions for Antibiotic Discovery. *Molecular Systems Biology* **2022**, *18* (9), e11081. https://doi.org/10.15252/msb.202211081.

(7) Scardino, V.; Filippo, J. I. D.; Cavasotto, C. How Good Are AlphaFold Models for Docking-Based Virtual Screening? **2022**. https://doi.org/10.26434/chemrxiv-2022-sgj8c.

(8) Zhang, Y.; Vass, M.; Shi, D.; Abualrous, E.; Chambers, J.; Chopra, N.; Higgs, C.; Kasavajhala, K.; Li, H.; Nandekar, P.; Sato, H.; Miller, E.; Repasky, M.; Jerome, S. Benchmarking Refined and Unrefined AlphaFold2 Structures for Hit Discovery. **2022**. https://doi.org/10.26434/chemrxiv-2022-kcn0d-v2.

(9) Alon, A.; Lyu, J.; Braz, J. M.; Tummino, T. A.; Craik, V.; O'Meara, M. J.; Webb, C. M.; Radchenko, D. S.; Moroz, Y. S.; Huang, X.-P.; Liu, Y.; Roth, B. L.; Irwin, J. J.; Basbaum, A. I.; Shoichet, B. K.; Kruse, A. C. Structures of the Σ2 Receptor Enable Docking for Bioactive Ligand Discovery. *Nature* **2021**, *600* (7890), 759–764. https://doi.org/10.1038/s41586-021-04175-x.

(10) Gorgulla, C.; Boeszoermenyi, A.; Wang, Z.-F.; Fischer, P. D.; Coote, P. W.; Padmanabha Das, K. M.; Malets, Y. S.; Radchenko, D. S.; Moroz, Y. S.; Scott, D. A.; Fackeldey, K.; Hoffmann, M.; Iavniuk, I.; Wagner, G.; Arthanari, H. An Open-Source Drug Discovery Platform Enables Ultra-Large Virtual Screens. *Nature*

2020, *580* (7805), 663–668. https://doi.org/10.1038/s41586-020-2117-z.

(11) Lyu, J.; Wang, S.; Balius, T. E.; Singh, I.; Levit, A.; Moroz, Y. S.; O'Meara, M. J.; Che, T.; Algaa, E.; Tolmachova, K.; Tolmachev, A. A.; Shoichet, B. K.; Roth, B. L.; Irwin, J. J. Ultra-Large Library Docking for Discovering New Chemotypes. *Nature* **2019**, *566* (7743), 224–229. https://doi.org/10.1038/s41586-019-0917-9.

(12) Bender, B. J.; Gahbauer, S.; Luttens, A.; Lyu, J.; Webb, C. M.; Stein, R. M.; Fink, E. A.; Balius, T. E.; Carlsson, J.; Irwin, J. J.; Shoichet, B. K. A Practical Guide to Large-Scale Docking. *Nat Protoc* **2021**, *16* (10), 4799–4832. https://doi.org/10.1038/s41596-021-00597-z.

(13) Trott, O.; Olson, A. J. AutoDock Vina: Improving the Speed and Accuracy of Docking with a New Scoring Function, Efficient Optimization, and Multithreading. *Journal of Computational Chemistry* **2010**, *31* (2), 455–461. https://doi.org/10.1002/jcc.21334.

(14) Eberhardt, J.; Santos-Martins, D.; Tillack, A. F.; Forli, S. AutoDock Vina 1.2.0: New Docking Methods, Expanded Force Field, and Python Bindings. *J. Chem. Inf. Model.* **2021**, *61* (8), 3891–3898. https://doi.org/10.1021/acs.jcim.1c00203.

(15) Alhossary, A.; Handoko, S. D.; Mu, Y.; Kwoh, C.-K. Fast, Accurate, and Reliable Molecular Docking with QuickVina 2. *Bioinformatics* **2015**, *31* (13), 2214–2216. https://doi.org/10.1093/bioinformatics/btv082.

(16) Li, H.; Leung, K.-S.; Wong, M.-H. Idock: A Multithreaded Virtual Screening Tool for Flexible Ligand Docking. In *2012 IEEE Symposium on Computational Intelligence in Bioinformatics and Computational Biology (CIBCB)*; 2012; pp 77–84. https://doi.org/10.1109/CIBCB.2012.6217214.

(17) Abagyan, R.; Totrov, M.; Kuznetsov, D. ICM—A New Method for Protein Modeling and Design: Applications to Docking and Structure Prediction from the Distorted Native Conformation. *Journal of Computational Chemistry* **1994**, *15* (5), 488–506. https://doi.org/10.1002/jcc.540150503.

(18) Halgren, T. A.; Murphy, R. B.; Friesner, R. A.; Beard, H. S.; Frye, L. L.; Pollard, W. T.; Banks, J. L. Glide: A New Approach for Rapid, Accurate Docking and Scoring. 2. Enrichment Factors in Database Screening. *J. Med. Chem.* **2004**, *47* (7), 1750–1759. https://doi.org/10.1021/jm030644s.

(19) Jones, G.; Willett, P.; Glen, R. C.; Leach, A. R.; Taylor, R. Development and Validation of a Genetic Algorithm for Flexible Docking11Edited by F. E. Cohen. *Journal of Molecular Biology* **1997**, *267* (3), 727–748. https://doi.org/10.1006/jmbi.1996.0897.

(20) Palacio-Rodríguez, K.; Lans, I.; Cavasotto, C. N.; Cossio, P. Exponential Consensus Ranking Improves the Outcome in Docking and Receptor Ensemble Docking. *Sci Rep* **2019**, *9* (1), 5142. https://doi.org/10.1038/s41598-019-41594-3.

(21) Preto, J.; Gentile, F. Assessing and Improving the Performance of Consensus Docking Strategies Using the DockBox Package. *J Comput Aided Mol Des* **2019**, *33* (9), 817–829. https://doi.org/10.1007/s10822-019-00227-7.

(22) Tuccinardi, T.; Poli, G.; Romboli, V.; Giordano, A.; Martinelli, A. Extensive Consensus Docking Evaluation for Ligand Pose Prediction and Virtual Screening Studies. *J. Chem. Inf. Model.* **2014**, *54* (10), 2980–2986.

https://doi.org/10.1021/ci500424n.

(23) Ochoa, R.; Palacio-Rodriguez, K.; Clemente, C. M.; Adler, N. S. DockECR: Open Consensus Docking and Ranking Protocol for Virtual Screening of Small Molecules. *Journal of Molecular Graphics and Modelling* **2021**, *109*, 108023. https://doi.org/10.1016/j.jmgm.2021.108023.

(24) Scardino, V.; Bollini, M.; Cavasotto, C. N. Combination of Pose and Rank Consensus in Docking-Based Virtual Screening: The Best of Both Worlds. *RSC Adv.* **2021**, *11* (56), 35383–35391. https://doi.org/10.1039/D1RA05785E.

(25) Sterling, T.; Irwin, J. J. ZINC 15 – Ligand Discovery for Everyone. *J. Chem. Inf. Model.* **2015**, *55* (11), 2324–2337. https://doi.org/10.1021/acs.jcim.5b00559.

(26) McGovern, S. L.; Shoichet, B. K. Information Decay in Molecular Docking Screens against Holo, Apo, and Modeled Conformations of Enzymes. *J. Med. Chem.* **2003**, *46* (14), 2895–2907. https://doi.org/10.1021/jm0300330.

(27) Lee, H. S.; Lee, C. S.; Kim, J. S.; Kim, D. H.; Choe, H. Improving Virtual Screening Performance against Conformational Variations of Receptors by Shape Matching with Ligand Binding Pocket. *J. Chem. Inf. Model.* **2009**, *49* (11), 2419–2428. https://doi.org/10.1021/ci9002365.

(28) Mysinger, M. M.; Carchia, M.; Irwin, John. J.; Shoichet, B. K. Directory of Useful Decoys, Enhanced (DUD-E): Better Ligands and Decoys for Better Benchmarking. *J. Med. Chem.* **2012**, *55* (14), 6582–6594. https://doi.org/10.1021/jm300687e.

(29) Evans, R.; O'Neill, M.; Pritzel, A.; Antropova, N.; Senior, A.; Green, T.; Žídek, A.; Bates, R.; Blackwell, S.; Yim, J.; Ronneberger, O.; Bodenstein, S.; Zielinski, M.; Bridgland, A.; Potapenko, A.; Cowie, A.; Tunyasuvunakool, K.; Jain, R.; Clancy, E.; Kohli, P.; Jumper, J.; Hassabis, D. Protein Complex Prediction with AlphaFold-Multimer. bioRxiv March 10, 2022, p 2021.10.04.463034. https://doi.org/10.1101/2021.10.04.463034.

(30) Mirdita, M.; Schütze, K.; Moriwaki, Y.; Heo, L.; Ovchinnikov, S.; Steinegger, M. ColabFold: Making Protein Folding Accessible to All. *Nat Methods* **2022**, *19* (6), 679–682. https://doi.org/10.1038/s41592-022-01488-1.

(31) Nichols, S. E.; Baron, R.; Ivetac, A.; McCammon, J. A. Predictive Power of Molecular Dynamics Receptor Structures in Virtual Screening. *J. Chem. Inf. Model.* **2011**, *51* (6), 1439–1446. https://doi.org/10.1021/ci200117n.

(32) Ravindranath, P. A.; Sanner, M. F. AutoSite: An Automated Approach for Pseudo-Ligands Prediction—from Ligand-Binding Sites Identification to Predicting Key Ligand Atoms. *Bioinformatics* **2016**, *32* (20), 3142–3149. https://doi.org/10.1093/bioinformatics/btw367.

(33) Spyrakis, F.; Cavasotto, C. N. Open Challenges in Structure-Based Virtual Screening: Receptor Modeling, Target Flexibility Consideration and Active Site Water Molecules Description. *Archives of Biochemistry and Biophysics* **2015**, *583*, 105–119. https://doi.org/10.1016/j.abb.2015.08.002.

(34) O'Boyle, N. M.; Banck, M.; James, C. A.; Morley, C.; Vandermeersch, T.; Hutchison, G. R. Open Babel: An Open Chemical Toolbox. *Journal of Cheminformatics* **2011**, *3* (1), 33. https://doi.org/10.1186/1758-2946-3-33.

(35) Schrödinger, LLC. The PyMOL Molecular Graphics System, Version 2.6.0a0 Open-Source, 2021.
(36) Truchon, J.-F.; Bayly, C. I. Evaluating Virtual Screening Methods: Good and Bad Metrics for the "Early Recognition" Problem. *J. Chem. Inf. Model.* **2007**, *47* (2), 488–508. https://doi.org/10.1021/ci600426e.
(37) Hunter, J. D. Matplotlib: A 2D Graphics Environment. *Computing in Science & Engineering* **2007**, *9* (3), 90–95. https://doi.org/10.1109/MCSE.2007.55.

Figure Legends

Figure 1. Virtual screening of protein structure in DUD-E database and AlphaFold. (a) Number distribution of protein categories of 51 targets selected from the DUD-E database. (b) Draw a semi-logarithmic ROC curve based on the virtual screening results of 51 targets by the AudoDock4 scoring function (λ= 0.001). The red curve depicts the screening result of protein structure in the DUD-E database, and the blue curve depicts the AlphaFold protein structure screening result. (c) 51 targets in autodock4, idock, qvina, rf_score, violin chart of screening results under the vinardo scoring function, using EF1%, AUC, logAUC, BEDROC (α= 80.5) indicators are used to evaluate the screening effect, among which red is the screening result of protein structure in DUD-E database, and blue is the screening result of AlphaFold protein structure. According to paired t-test, two groups of data (red and blue) with the same scoring function and the same indicator have been marked with p values that are statistically different. ** represents $p<0.01$, and * represents $p<0.05$.

Figure 2. Binding pocket structure and virtual screening results of Holo, AlphaFold and Apo protein structures. (a-b) Water molecules have been removed from protein structures. AlphaFold structure and Apo (obtained from PDB database) structure are aligned with Holo (obtained from DUD-E database) structure, displayed in grid form, and cut the same section. Green is Holo structure, purple is AlphaFold

structure, and yellow is Apo structure. PyMOL is used for operation and drawing. HIVRT (a) and AKT2 (b) protein structures of Holo, AhphaFold and Apo three-dimensional grid diagram sections were displayed. (c) 23 targets in autodock4, idock, rf_score, violin chart of screening results under the vinardo scoring function, using EF1%, AUC, logAUC, BEDROC (α= 80.5) indicators are used to evaluate the screening effect. Among them, red group represent the screening result of protein structure (Holo) in DUD-E database, blue group represent screening result of AlphaFold protein structure, and green is the screening result of Apo protein structure. Three groups of data (red, blue and green) with the same scoring function and the same indicator are all marked according to paired t-test, and those with statistically different. ** represents $p<0.01$, and * represents $p<0.05$.

Figure 3. Evaluation of consensus scoring method based on score or ranking. (a) According to the DUD-E database, 51 targets are uploaded into autodock4, idock, qvina, rf_ Score and vinardo are the screening results of five scoring functions. Scatter plots and fitting lines are drawn between different scoring functions. The red is logAUC, and the blue is BEDROC (α= 80.5). (b) According to DUD-E database, BACE1 target is used as an example to draw scatter plots of four consensus scoring methods: exp_z_score, sum_rank, best_rank, and worst_rank (all with idock and rf_score as inputs). The abscissa is the ranking of small molecules in idock, and the ordinate is the ranking of small molecules in rf_score, in which that gray and silver are decoys, red and purple are actives, and silver and purple are the top 10% of the ranking obtained by the corresponding consensus scoring method. (c) The 51 targets in the DUD-E database screen the violin chart of the results under 4 single scoring functions (blue) and 13 consensus scoring methods (red, with autodock4, idock, rf_score, vinardo as the input), and use EF1%, AUC, logAUC, BEDROC (α= 80.5) indicators are used to evaluate the screening effect. The x-axis scoring function is sorted by the average value of logAUC, with marked exp_z_score corresponding to the upper limit and lower limit of the data (gray dotted line), quartile (green dotted line), and median (blue dotted line).

Figure 4. Re-evaluation of Holo, AlphaFold and Apo protein structures using consensus scoring method. (a-b) We used four consensus scoring methods (all with autodock4, idock, rf_score, vinardo as input): exp_ z_score, sum_rank, best_rank and worst_rank. And EF1%, AUC, logAUC, BEDROC (α= 80.5) indicators are used to evaluate the screening effect. Panel (a) showed screening results of DUD-E protein structure (red) and AlphaFold protein structure (blue) of 51 targets in DUD-E database. Panel (b) showed screening results of DUD-E protein structure (red), AlphaFold protein structure (blue) and Apo protein structure (green) of 23 targets in DUD-E database. (c) 51 protein targets by exp_z_score were used to count the difference of AUC, logAUC, BEDROC (α= 321.9, α= 80.5, and α= 20.0) and EF (1%, 5%, and 10%) between DUD-E database and AlphaFold protein structure. Negative number (red) indicates that the structure of AlphaFold protein is worse than that of DUD-E protein, and positive number (blue) indicates that the structure of AlphaFold protein is better than that of DUD-E protein. The difference of logAUC sorts the data in the table. There are 20 targets (about 39% of protein targets) whose difference of logAUC is less than -0.03. There are 18 (about 35%) targets whose difference of logAUC is greater than -0.03, and less than or equal to 0.03. There are 13 targets (about 25%) with a difference of logAUC greater than 0.03.

Figure 5. Multi-stage screening combined with consensus scoring. (a) Multi-stage screening flow chart combined with consensus scoring. Prepare small molecules, proteins and search space, and then start multi-stage screening. In the first stage, idock docking is used for virtual screening to obtain idock rank and rf_score rank, and then ir rank is obtained through the consensus score of idock rank and rf_score rank. The top x% of the ir rank are taken to enter the second stage. In the second stage, we use the vinardo scoring function to conduct virtual screening to obtain the vinardo rank, and then take the small molecules in the topx% of the ir rank in the idock rank and rf_score rank and all the small molecules in the vinardo rank for consensus scoring to obtain the irv rank. The top y% of the irv rank are taken to enter the third stage. In the

third stage, the autodock4 scoring function is used to conduct virtual screening, and the autodock4 rank is obtained. Then the small molecules in idock rank, rf_score rank and vinardo rank that are y% before irv rank and all small molecules in autodock4 rank are scored by consensus to obtain irva rank. The final ranking is obtained by ranking the small molecules in irva rank, the small molecules in irv rank that are not in irva rank, and the small molecules in irv rank that are not in irv rank according to the original order within the ranking. (b) 51 targets in DUD-E database are in exp_z_score consensus scoring (all with autodock4, idock, rf_score, vinardo as input). We integrated multi-stage screening with consensus scoring (plan A, C, E), multi-stage screening without consensus scoring (plan B, D, F, the flow chart is shown in Supplementary Information Figure 1) and screening results under a single scoring function (autodock4, idock, rf_score, vinardo). The average time of small molecules of each target in 51 targets (blue, unit: second/cpu/molecule), and the average time of small molecules of all targets in 51 targets (green, unit: second/cpu/molecule). (c) 51 targets in DUD-E database are in exp_z_score Consensus scoring (all with autodock4, idock, rf_score, vinardo as input), multi-stage screening with consensus scoring (plan A, C, E), and multi-stage screening without consensus scoring (plan B, D, F). The violin charts demonstrated screening results of EF1%, AUC, logAUC and BEDROC (α= 80.5). For plan A and plan B, take top 40% in the first stage to enter the second stage, and take top 50% in the second stage to enter the third stage. In the first stage of plan C and plan D, take top 20% to enter the second stage, and in the second stage, take top 50% to enter the third stage. Plan E and plan F take top 10% in the first stage to enter the second stage, and take top 50% in the second stage to enter the third stage.

Figure 6. Relationship between scoring score and hit rate. (a-j) The hit rate of 51 targets by Autodock4, idock, rf, vinardo and exp_z_score. The red dotted lines represent total active small molecules/total small molecules, the rate of each subgraph is about 3.0%. The gray dotted lines represent the number of small molecules. The green dotted lines represent the total hit rate. The blue dotted lines represent the average hit rate of 51 targets. The light gray dotted lines represent the hit rate of each

target of 51 targets. The abscissa of a, b, c, e, f, g, i, j were divided into 22 segments according to the score, of which the end two segments respectively contain data that is greater than or equal to and less than the boundary, and the remaining 20 segments contain data that is left closed and right open within the segment. The abscissa of d and h were divided into 21 segments according to the score. One segment at the right end contains data that is greater than or equal to the boundary, and the other 20 segments contain data that is left closed and right open within the segment. A, b, c, d, i are the screening results of protein structure in the DUD-E database, and e, f, g, h, j are AlphaFold protein structure screening results.

Figures

Figure 1

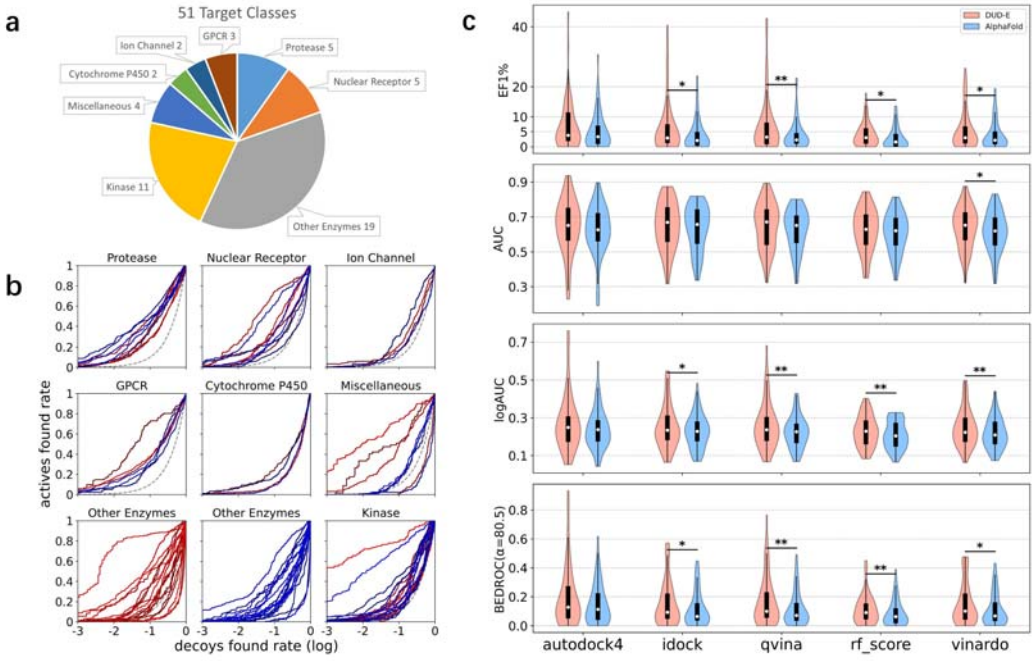

Figure 2

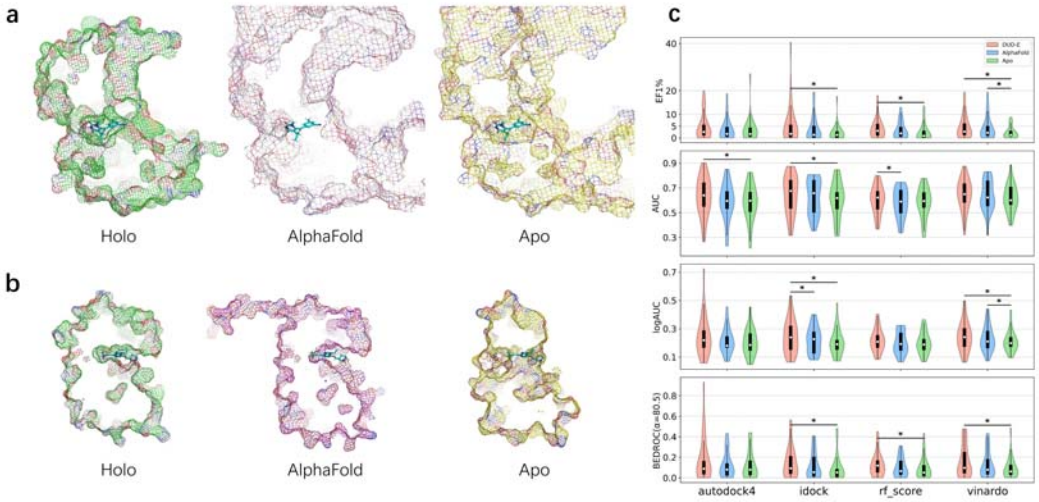

Figure 3

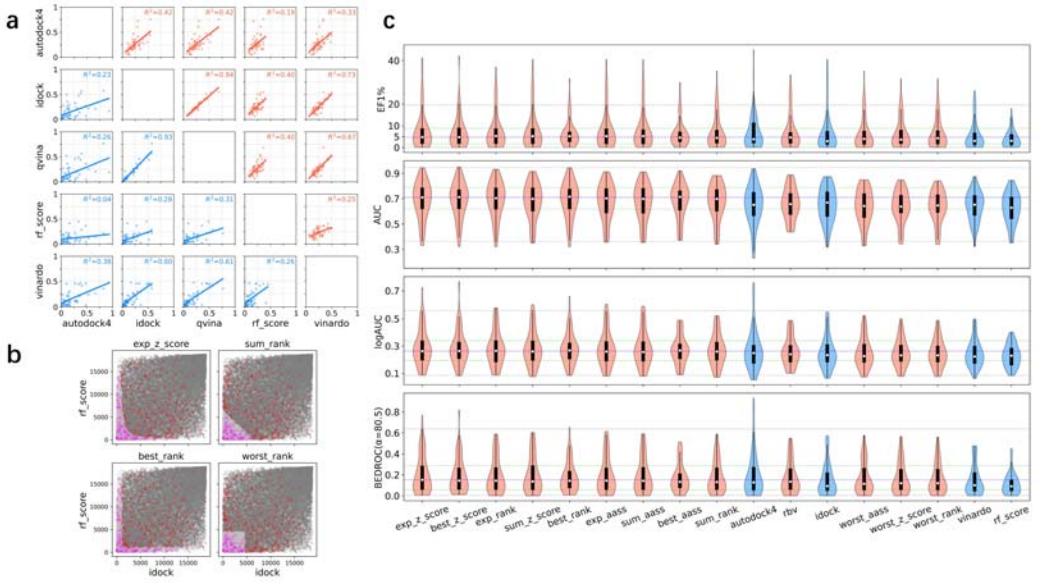

Figure 4

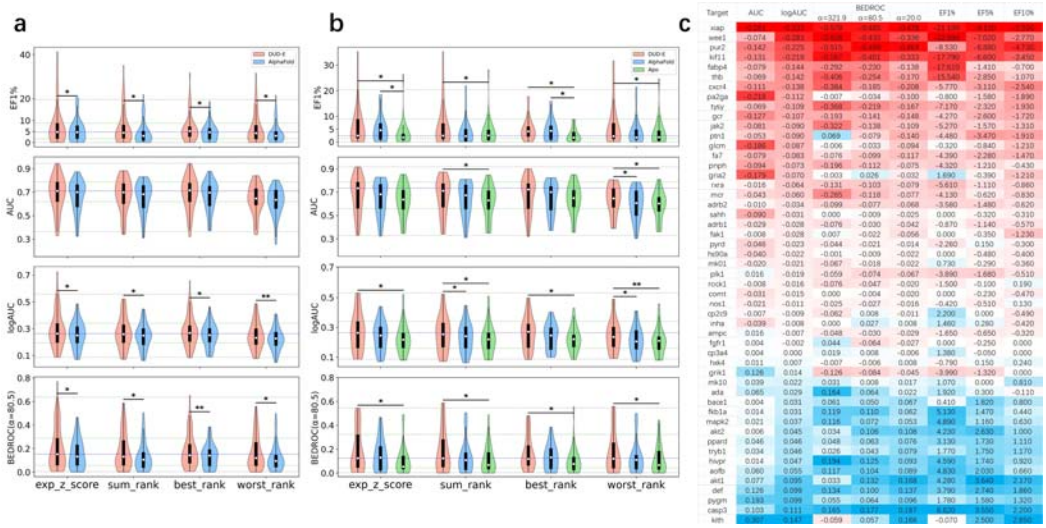

Figure 5

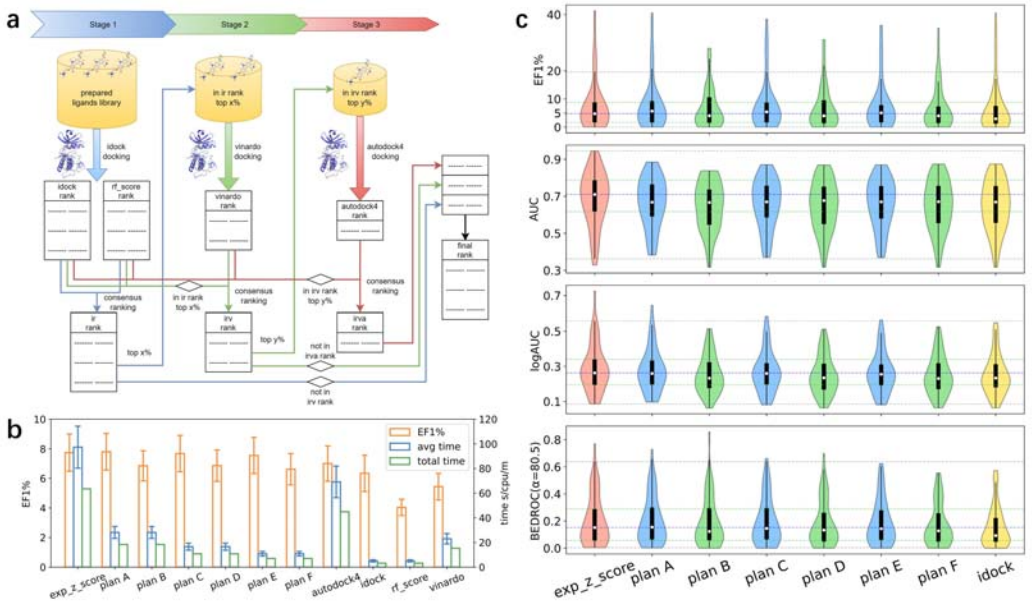

Figure 6

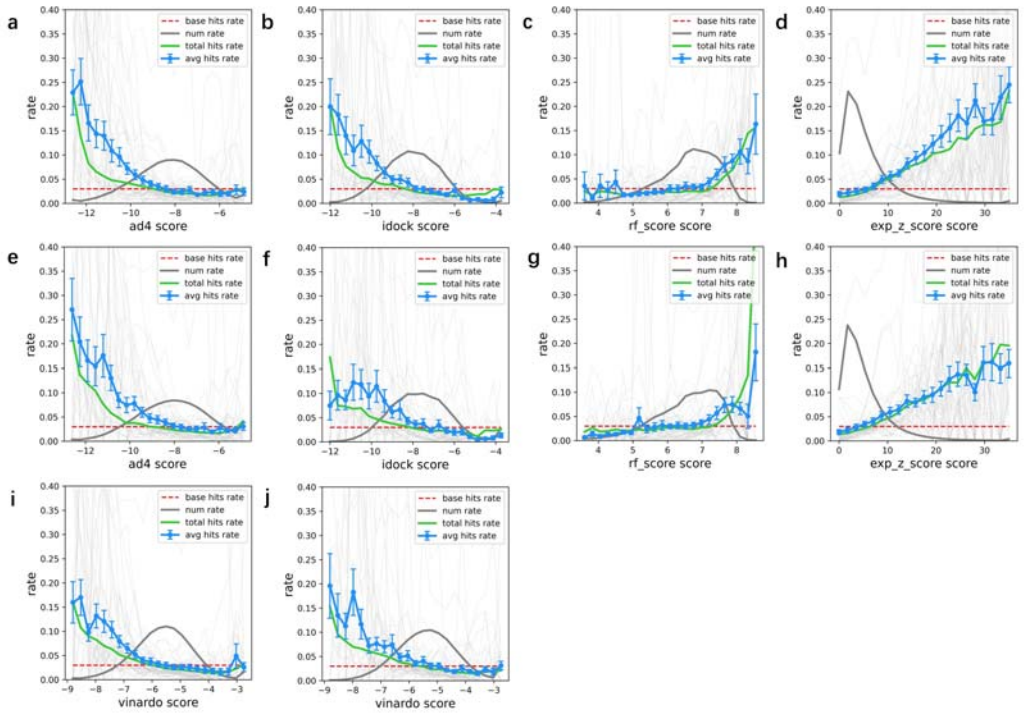

Tables

Table 1. Virtual screening results of protein structure in DUD-E database and AlphaFold.

	AUC	logAUC	BEDROC(α =321.9)	BEDROC(α =80.5)	BEDROC(α =20.0)	EF1%	EF5%	EF10 %
AF ad4	0.622	0.240	0.183	0.150	0.196	5.284	3.238	2.522
AF idock	0.635	0.228	0.126	0.114	0.166	3.985	2.624	2.226
AF rf_score	0.609	0.208	0.087	0.086	0.140	2.961	2.254	1.984
AF vinardo	0.614	0.217	0.128	0.109	0.157	3.892	2.531	2.105
DUD-E ad4	0.645	0.270	0.229	0.194	0.235	7.002	3.915	2.896
DUD-E idock	0.647	0.252	0.204	0.156	0.199	6.342	3.235	2.574
DUD-E rf_score	0.625	0.228	0.118	0.116	0.172	4.040	2.865	2.336
DUD-E vinardo	0.639	0.245	0.172	0.152	0.198	5.436	3.282	2.509

The average value for 51 targets of AUC, logAUC, BEDROC (α= 321.9, α= 80.5, and α= 20.0), EF1%, EF5%, and EF10% were used to evaluate the screening results. AF is

the abbreviation of AlphaFold, indicating the use of AlphaFold protein structure. DUD-E represents the use of the DUD-E database protein structure. Ad4 means using the autodock4 scoring function, idock means using the idock scoring function, rf_score means using the rf_score scoring function in the idock software, and vinardo means using the vinardo scoring function.

Table 2. Virtual screening results of Holo, AlphaFold, Apo protein structure.

	AUC	logAUC	BEDROC(α =321.9)	BEDROC(α =80.5)	BEDROC(α =20.0)	EF1%	EF5%	EF10 %
AF ad4	0.587	0.212	0.141	0.121	0.167	3.638	2.497	2.100
AF idock	0.625	0.220	0.129	0.115	0.161	3.700	2.291	2.020
AF rf_score	0.576	0.200	0.103	0.101	0.148	3.330	2.439	1.951
AF vinardo	0.633	0.230	0.152	0.126	0.176	4.183	2.622	2.306
Apo ad4	0.580	0.206	0.124	0.122	0.164	3.593	2.396	2.029
Apo idock	0.603	0.202	0.093	0.089	0.139	2.308	2.104	1.797
Apo rf_score	0.581	0.198	0.099	0.092	0.146	2.440	2.249	1.955
Apo vinardo	0.617	0.210	0.074	0.095	0.157	2.311	2.466	2.035
DUD-E ad4	0.628	0.248	0.191	0.172	0.212	4.757	3.267	2.505
DUD-E idock	0.641	0.244	0.179	0.147	0.196	5.455	3.025	2.436
DUD-E rf_score	0.603	0.218	0.134	0.127	0.171	4.016	2.804	2.164
DUD-E vinardo	0.645	0.245	0.171	0.160	0.207	4.667	3.333	2.583

The average value for 51 targets of AUC, logAUC, BEDROC (α= 321.9, α= 80.5, and α= 20.0), EF1%, EF5%, and EF10% were used to evaluate the screening results. AF is the abbreviation of AlphaFold, indicating the use of AlphaFold protein structure. DUD-E represents the use of the DUD-E database protein structure. Ad4 means using the autodock4 scoring function, idock means using the idock scoring function, rf_score means using the rf_score scoring function in the idock software, and vinardo means using the vinardo scoring function.

Table 3. Evaluation consensus scoring method based on score or ranking.

	AUC	logAUC	BEDROC(α =321.9)	BEDROC(α =80.5)	BEDROC(α =20.0)	EF1%	EF5%	EF10%
exp_z_score	0.686	0.290	0.248	0.204	0.253	7.736	4.226	3.202
best_z_score	0.687	0.285	0.222	0.193	0.246	7.038	4.162	3.101
exp_rank	0.689	0.284	0.247	0.193	0.244	7.423	4.047	3.104
sum_z_score	0.676	0.282	0.250	0.197	0.243	7.697	4.059	3.068
best_rank	0.688	0.280	0.187	0.180	0.243	6.533	4.138	3.118
exp_aass	0.671	0.279	0.248	0.195	0.240	7.617	3.982	3.021
sum_aass	0.669	0.278	0.248	0.194	0.238	7.506	3.955	2.971
best_aass	0.678	0.272	0.192	0.173	0.230	6.356	3.893	2.998
sum_rank	0.673	0.272	0.234	0.179	0.227	6.782	3.722	2.901
ad4	0.645	0.270	0.229	0.194	0.235	7.002	3.915	2.896
rbv	0.659	0.260	0.211	0.171	0.223	6.735	3.636	3.003
idock	0.647	0.252	0.204	0.156	0.199	6.342	3.235	2.574
worst_aass	0.633	0.250	0.204	0.164	0.206	6.187	3.430	2.608
worst_z_score	0.634	0.249	0.223	0.166	0.204	6.366	3.363	2.534
worst_rank	0.635	0.249	0.223	0.164	0.202	6.258	3.297	2.507
vinardo	0.639	0.245	0.172	0.152	0.198	5.436	3.282	2.509
rf_score	0.625	0.228	0.118	0.116	0.172	4.040	2.865	2.336
p value	0.054	0.075	0.961	0.102	**0.028**	0.399	0.068	**0.028**

The average value for 51 targets of AUC, logAUC, BEDROC (α= 321.9, α= 80.5, and α= 20.0), EF1%, EF5%, and EF10%were used to evaluate the screening results . Ad4 means to use the autodock4 scoring function, idock means to use the idock scoring function, rf_score means to use rf_score scoring function in idock software, and vinardo means to use vinardo scoring function. In the last line, p-value is the result of paired t-test on exp_z_score index data and exp_rank (ECR) index data. The data ($p<0.05$) has been bold. The remaining data are the screening results of consensus scoring method.

Table 4. Evaluation of Holo, AlphaFold protein structure using consensus scoring methods.

	AUC	logAUC	BEDROC(α =321.9)	BEDROC(α =80.5)	BEDROC(α =20.0)	EF1%	EF5%	EF10%
DUD-E	0.686	0.290	0.248	0.204	0.253	7.736	4.226	3.202
AF	0.665	0.256	0.164	0.151	0.208	5.518	3.547	2.744
AF - DUD-E	-0.021	-0.034	-0.084	-0.053	-0.045	-2.218	-0.679	-0.458
p value	0.129	**0.014**	**0.004**	**0.014**	**0.024**	**0.020**	0.068	**0.043**

The screening results of consensus score exp_z_score (with autodock4, idock, rf_score, vinardo as input) show as AUC, logAUC, BEDROC (α= 321.9, α= 80.5, and α= 20.0), EF1%, EF5%, and EF10% on 51 targets. The line named DUD-E means the average of 51 structures in DUD-E database. The line named AlphaFold means the average of 51 AlphaFold structures. The line named AF – DUD-E means the average of 51 AlphaFold structures minus the average of 51 structures in DUD-E database. The line named p value is the paired t-test for each index data of DUD-E (Holo) and AlphaFold protein structure screening results. The data ($p<0.05$) has been thickened.

Table 5. Evaluate the protein structure of Holo, AlphaFold and Apo using consensus scoring methods.

	AUC	logAUC	BEDROC(α =321.9)	BEDROC(α =80.5)	BEDROC(α =20.0)	EF1%	EF5%	EF10%
DUD-E	0.671	0.271	0.218	0.189	0.237	6.295	3.644	2.918
AF	0.641	0.241	0.169	0.147	0.197	5.161	3.128	2.473
Apo	0.627	0.223	0.103	0.110	0.170	3.223	2.624	2.223
AF - DUD-E	-0.030	-0.030	-0.049	-0.042	-0.040	-1.134	-0.516	-0.445
AF - Apo	0.014	0.018	0.066	0.037	0.026	1.938	0.504	0.249
Apo - DUD-E	-0.044	-0.049	-0.115	-0.079	-0.067	-3.072	-1.020	-0.694
AF DUD-E p value	0.082	0.060	0.192	0.145	0.118	0.294	0.223	0.128
AF Apo p value	0.398	0.243	0.119	0.136	0.233	**0.050**	0.251	0.364
Apo DUD-E p	0.052	**0.020**	**0.021**	**0.019**	**0.029**	**0.011**	0.064	0.055

value								

The screening results of exp_z_score consensus score (with autodock4, idock, rf_score, vinardo as input) show as AUC, logAUC, BEDROC (α= 321.9, α= 80.5, and α= 20.0), EF1%, EF5%, and EF10% on 23 targets. The results of using DUD-E database protein structure, AlphaFold (AF) protein structure, Apo protein structure, AlphaFold minus DUD-E (AF - DUD-E), AlphaFold minus Apo (AF - Apo), and Apo minus DUD-E (Apo – DUD-E) are displayed line by line. P-value is the paired t-test for each index data of DUD-E (Holo), AlphaFold, and Apo protein structure screening results, respectively. The data of $p<0.05$ has been thickened.

Table 6. Early enrichment capacity and time of multi-stage screening combined with consensus score.

	exp_z_score	plan A	plan B	plan C	plan D	plan E	plan F	autodock4	idock	rf_score	vinardo
EF1%	7.74	7.80	6.85	7.68	6.86	7.55	6.62	7.00	6.34	4.04	5.44
avg time	97.34	28.17	28.17	16.65	16.65	10.89	10.89	69.19	5.13	5.13	23.03
total time	63.51	18.38	18.38	10.82	10.82	7.04	7.04	44.93	3.26	3.26	15.31

EF1% indicators of the screening results of 51 targets in the DUD-E database under exp_z_score consensus score (all with autodock4, idock, rf_score, vinardo as input), multi-stage screening (plan A, C, E) combined with consensus score, multi-stage screening (plan B, D, F) without consensus score, and single scoring function (autodock4, idock, rf_score, vinardo). The average small molecule average time of each target in 51 targets (avg time, unit: second/cpu/molecule), and the average small molecule average time of all targets in 51 targets (total time, unit: second/cpu/molecule).